A New Dynamical Reference Point Adaptation Mechanism in indicator-based EMOA based on weak convergence detection

Weiduo Liao, Ke Shang and Hisao Ishibuchi
Department of Computer Science and Engineering
Southern University of Science and Technology, Shenzhen, China
Email: 11849249@mail.sustech.edu.cn
kshang@foxmail.com
hisao@sustech.edu.cn

***Abstract*—In the field of indicator-based evolutionary multi-objective optimization algorithms(indicator-based EMOAs), hypervolume is a popular indicator, which is the only pareto-compliant indicator up to now. But recently, a paper shows that the position of reference point will influence the diversity of the final solutions of hypervolume-based EMOAs when applying to the inverted-triangular pareto front problems, by influencing the hypervolume contribution of the external solutions. In this paper, we state this phenomenon and introduce the reference point adaptation with a dynamic mechanism in terms of necessity. Then we propose a new dynamic mechanism based on weak convergence detection. In our approach, the simple Least Squares and the information of nadir point are used to detect the convergence. After that, we examine the difference between this new dynamic mechanism with a state-of-the-art linearly decrease mechanism.**

***Keywords*—reference point adaptation; indicator-based algorithm; hypervolume; evolutionary multi-objective optimization; behavior; dynamic mechanism; convergence detection**

I. Introduction

In the field of evolutionary multi-objective optimization algorithms (EMOAs), several researchers focus on various indicators including hypervolume [1], R2 [2], ϵ_+ indicator [3] and IGD [4]. The indicators are designed for different purposes, and as a matter of fact, have their own strong points and drawbacks. Different from IGD, hypervolume does not need the pre-knowledge of the shape of the pareto front and is the only pareto-compliant indicator up to now [5]. But with a heavy computation load of hypervolume computation [6], the hypervolume-based algorithms get poor performances in running time when dealing with problems which have more than three objectives, which is so-called Many-Objective Optimization Problems(MaOPs).

In order to reduce the heavy computation cost of hypervolume computation, many new indicators or new methods have been proposed to estimate the hypervolume. For example, HypE use a Monte Carlo simulation technology to estimate the effect of hypervolume [7]; R2 indicator bases on a standard weighted Tchebycheff function [2] and a new R2 is proposed by Shang et al [8]. Recently, an improved SMS-EMOA with adaptive resource allocation has been proposed to reduce the number of hypervolume calculations [9]; In 2015, a simple and fast version of SMS-EMOA [10], so-called FV-EMOA, has been proposed [11]. In order to further reduce the bottleneck of high time complexity for calculating the hypervolume contributions, the FV-EMOA considers the fact that the hypervolume contribution of a single solution is only associated with partial solutions rather than the whole solution set [11]. Based on this point, the FV-MOEA reduces the computational cost greatly. In this paper, the FV-MOEA is used in the experiment section, for its better performance on time-saving than SMS-EMOA [11].

The specification of the reference point is one of the important parts in hypervolume computation. It has been reported that the position of reference point strongly influences the value of hypervolume contribution of the external solutions on the problems with inverted-shape pareto fronts [12]–[14]. A suitable set of reference point position for flat pareto fronts has been sufficiently investigated in Hisao st al [13]. And a dynamic reference point adaptation has also been proposed in Hisao st al [15]. Another strategy proposed is to use two reference points in hypervolume-based EMOA [16]. In this paper, the dynamic mechanism is stated in two different stages of the algorithm running process. At the early stage, for a better searching behavior of the algorithm, the reference point should be set a little worse than the suggested position at the beginning. Then by a dynamic mechanism, the reference point is gradually decreasing to the suggested position following the iteration.

After that, we propose a new dynamic reference point adaptation with a weak convergence detection in hypervolume-based EMOA. The simple least squares and the logarithm value of nadir point as a convergence indicator are used in this weak convergence detection. For a given window w_l genera-

This work was supported by the Program for Guangdong Introducing Innovative and Entrepreneurial Teams (Grant No. 2017ZT07X386), Shenzhen Peacock Plan (Grant No. KQTD2016112514355531), the Science and Technology Innovation Committee Foundation of Shenzhen (Grant No. ZDSYS201703031748284), the Program for University Key Laboratory of Guangdong Province (Grant No. 2017KSYS008), and National Natural Science Foundation of China (Grant No. 61876075).

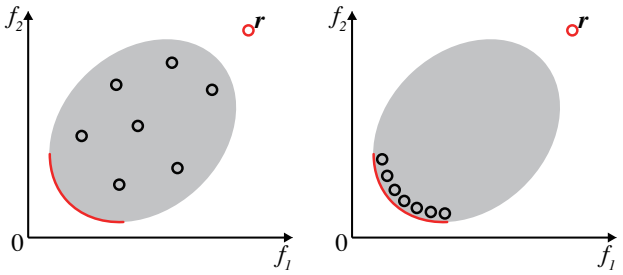

(a) The initial generation. (b) The final generation.

Fig. 1: The reference point is set with a large feasible space. pareto front can be far away from reference point. The gray region shows the feasible region and the red arc is the corresponding pareto front. The red circle r is the reference point calculated by the initial solutions in (1a) which is randomly generated. After some generations, the current solutions reach to the five black circles in (1b), which is far away from the reference point.

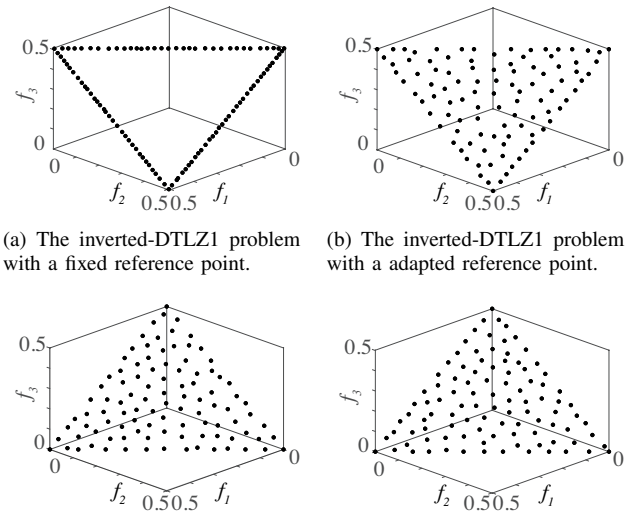

(a) The inverted-DTLZ1 problem with a fixed reference point.

(b) The inverted-DTLZ1 problem with a adapted reference point.

(c) The DTLZ1 problem with a fixed reference point.

(d) The DTLZ1 problem with a adapted reference point.

Fig. 2: The final distribution of solutions set in the inverted-DTLZ1(2a and 2b) and the DTLZ1 problem(2c and 2d). The algorithm is FV-EMOA with population size $= 100$, evaluation number $= 20000$ and $r = 1.1$. (2a and 2c): the reference point is calculated only once at the initial step; (2b and 2d): the reference point is adapted based on the formula (1). All the solutions in the final distribution are at the boundary of the pareto front in (2a), which shows the bad effect of a faraway reference point on the final distribution of inverted-triangular problems. This bad effect can not be observed on triangular problems in (2c).

tions, if the slope of linear regression is below one threshold, we report the convergence. The comparison of two dynamic mechanisms and simple reference point adaptation(without dynamic mechanism) is discussed in the experiment section. On some specific conditions, for example, when the total evaluation number is limited to a small addition after the reported convergence, our weak convergence detection mechanism outperforms the linearly decrease mechanism.

The remainder of this paper is organized as follows. Firstly, we briefly introduce the basic idea of reference point adaptation by a simple example in Section II. Then, we state the reference point adaptation with the dynamic mechanism in Section III. The necessity of a dynamic mechanism is also illustrated in this Section. After that, the details of the new dynamic mechanism proposed in this paper is in Section IV. And we report our computational experiments of FV-EMOA with several triangular and inverted-triangular problems in Section V. our experiments are performed on 3- and 5-dimension problems for clearly comparing of two dynamic mechanisms and simple reference point adaptation (without dynamic mechanism). Finally, the conclusion is shown in Section VI.

II. Reference Point Adaptation

When hypervolume(HV) is used in indicator-based algorithms, one important thing to be considered is how to specify the reference point. Before calculating the HV values, a reference point needs to be chosen in advance. However, it is not suggested that the reference point is set only once at the beginning. This may cause a very far away reference point from solutions for those problems with a very large feasible space(As shown in Fig. 1), as the solutions set is gradually converging to the pareto front during the iteration of the algorithm process.

There is a big problem when applying this strategy to some problems with specific pareto front shape, for example, the inverted-DTLZ1 problem with an inverted-triangular pareto front in 3 dimensions, that many solutions in the final solutions set will distribute at the boundary of the pareto front (Fig. 2a comparing with Fig. 2b) [13]–[15]. Although it has no effect on the distributions of solutions set in problems with triangular pareto front in 3 dimensions (Fig. 2c comparing with Fig. 2d), it is necessary using reference point adaptation during the algorithm progress. And the reason is illustrated detailedly in Hisao et al [14].

In many algorithms including SMS-EMOA [10], the reference point is adapted based on the following rules:

$$RP = r * ENP, r = 1.1. \tag{1}$$

Note that the estimated nadir point(ENP) is the nadir point in current population. When the solutions in the current population are obtained, we use hypervolume as the indicator to evaluate the performance of the solutions set. Then the reference point used to calculate the hypervolume is calculated by the formula above.

III. Dynamic Mechanism

Basically, the process of Evolutionary Multi-objective Optimization Algorithm can be separated into two stages:

1) Early Stage: In this stage, all the solutions are far away from pareto front. The main task is to converge the solutions to pareto front. We also call this stage the convergence stage.

2) Final Stage: In this stage, all the solutions are in or near the pareto front. So the main task is to make the distribution of solutions more evenly in the pareto front. We also call this stage the diversity stage.

For different purposes in these two stages, the r should be treated differently [15]. Not only the reference point but also the value of r needs to be adapted in each iteration of the algorithm. This is called dynamical reference point adaptation.

Unfortunately, the research on how to specified r is limited. Only a few papers [12]–[14] did some research on the optimal setting of the reference point on flat (not concave or convex) pareto front problems. The reason is that the effect of the location of the reference point on the pareto front is not fatal on some benchmark problems, especially triangular pareto front. But in fact, on some specific problems, the distribution of solutions on pareto front strongly depends on the location of the reference point. The sensitivity about the value of r for solutions is also observed on some real-world problems, for example, distance minimization problems. This observation potential shows the usefulness of the dynamical reference point adaptation [15].

In this section, we will specify the suggested r values separately in the early and final stages.

A. Reference Point Specification for Optimal Distribution

In the final stages, the major purpose is to augment the diversity of solutions set. More specifically, for inverted-triangular problems, in order to have same hypervolume contribution, the interval between two boundary solutions should be the same as that between two inner solutions. In hisao st al [12], the suggested value of r for flat(not concave or convex) pareto front problems is:

$$r = 1 + \frac{1}{H}, \tag{2}$$

as shown in Fig. 3. H is the number of solutions intervals in 2-dimension and the number of interval at each boundary of pareto front in many-dimension. In Fig. 3a, $r = 1.2(H = 5)$ is the optimal setting for a 21 individuals inverted-DTLZ1 problem and a evenly distribution is observed. In Fig. 3b - Fig. 3d, the inner solutions are decreased and move to the boundary of pareto front.

For simple illustration, when algorithm reaches to the final stage, all solutions are near the pareto front, r should be specified as $1 + 1/H$, as in equation 2.

B. Reference Point Specification for Better Searching Behavior

However, in the early stage, solutions set is not close to the pareto front, which makes the estimated ideal and nadir points far away from true ideal and nadir points, for the reason that they are calculated by current solutions in each generation. And considering some problems without an easy mapping from decision space to objective space, if the external solutions have the same hypervolume contribution with the inner solutions, the exploration of pareto front will be poor. As a result, the solutions can hardly jump out from the local minimums and the diversity will be poor. Two examples are given in the experiment section (As shown in Fig. 6d and 7d).

In [15], a larger value of r than the $1 + 1/H$ is suggested in the early stage.

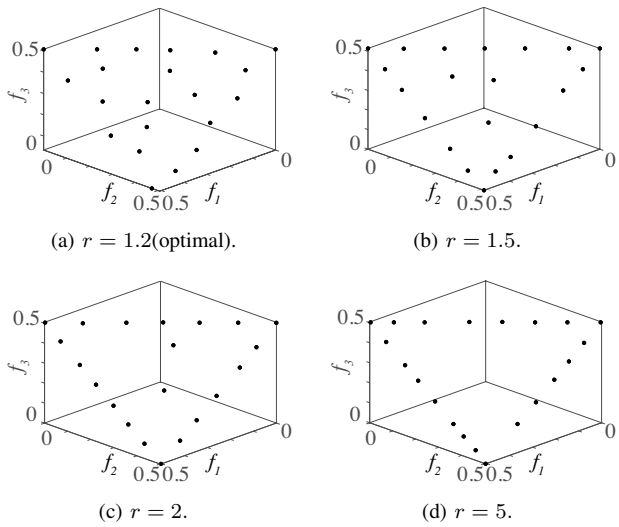

(a) $r = 1.2$(optimal). (b) $r = 1.5$. (c) $r = 2$. (d) $r = 5$.

Fig. 3: The final distribution of solutions set in the inverted-DTLZ1 problem. The algorithm is FV-EMOA with population size $= 21(H = 5)$ and evaluation number $= 20000$. $r = 1.2$ is the optimal setting and we observed a evenly distribution in (3a). As the increasing of r, solutions are more likely to be at the boundary (3b-3d).

C. Linearly Decrease Mechanism

Based on the theory above, r is suggested to be specified dynamically at different stages of the algorithm(at early stage, a slightly larger r is chosen; at final stage, $r = 1 + 1/H$ is chosen). But unfortunately, there is no best mechanism on how to specify the value of r dynamically outperforms the others in all problems and all experiment settings. One mechanism may be the best when working on some specific experiment conditions, but may not be good on other conditions.

In [15], a linearly decrease mechanism has been proposed:

$$r(t) = r_{Initial}\frac{(T-t)}{T} + (1 + 1/H)\frac{t}{T}, t = 0, 1, \ldots, T, \tag{3}$$

where T is the total number of generations, and $r_{Initial}$ is the initial value of r, which is larger than $1 + 1/H$. It is a simple and practical mechanism. In (3), the value of r starts from $r_{Initial}$, then gradually decreases to the suggested value in a linearly decrease process.

In the next section, we will propose another good dynamic mechanism based on weak convergence detection criterion outperforms simple linearly decrease mechanism on some constraint condition.

IV. New Dynamic Mechanism

In this section, we will introduce a new mechanism that uses a weak convergence detection criterion to decide whether to change the value of r from $r_{Initial}$ to $1 + 1/H$.

As we have explained before, a slightly larger r is suggested at the initial stage of the algorithms. But for good diversity at the final stage, it is needed to set r to its optimal value $(1 + 1/H)$. For this purpose, we detect whether the algorithm is converged or not. If solutions are all close to the pareto front, we change the value of r to $r_{Optimal}$; otherwise, we set value of r to $r_{Initial}$. The mechanism is also shown below:

$$\begin{aligned} r(t) = r_{Initial}\mathbb{I}\left[t < t_{Convergent}\right] \\ + (1 + 1/H)\mathbb{I}\left[t \geq t_{Convergent}\right], t = 0, 1, \ldots, T, \end{aligned} \tag{4}$$

where $\mathbb{I}$ is the indicator function returning 1 if argument is true and 0 otherwise. $r(t)$ equals to $r_{Initial}$ before reaching to the convergent generation $t_{Convergent}$, and changes to $1 + 1/H$ after $t_{Convergent}$. The $t_{Convergent}$ is determined by a weak convergence detection criterion.

A. Weak Convergence Detection

Consider many convergence detection papers [17]–[23], various indicators including convergence detection indicators are using to detect the stagnation. They focus on the accuracy of convergence, which is not the purpose in our approach for the reason that after algorithm convergent, we still need some generations in order to get even distribution of solutions set. We summarize our weak convergence detection criterions as follow:

1) inaccuracy: It is no need to have an accurate convergence detection. The convergence can be reported if current solutions are close to the pareto front. In other words, the estimated ideal and nadir points based on the current solutions are close to the true ideal and nadir points.

2) saving time: We should not spend too much time in convergence detection for the reason that the state-of-the-art indicator-based algorithms such as SMS-EMOA and HypE, are time-consuming when the dimension is very high.

We are discussing the effect of reference points in calculating hypervolume. It seems to be a good idea to use progress indicator hypervolume as our convergence detection indicator, for that, we have calculated hypervolume in each generation in the hypervolume-based evolutionary multi-objective optimization algorithm. But during the process of algorithm, the reference point is calculated by (1) in each generation. So we can not just simply compare hypervolume calculated in algorithm among different generations.

We are trying on some other good indicators satisfying our convergence detection criterions. Fig. 4 shows the change of hypervolume(HV) and nadir point on the FV-EMOA algorithm with the 3-dimensional inverted-DTLZ1 problem. When current solutions are close to the pareto front, the estimated nadir point is close to the true nadir points. This implies that the estimated nadir point can be a good indicator of our purpose. But for some problems with the large feasible region, the moving distance of the estimated nadir point in

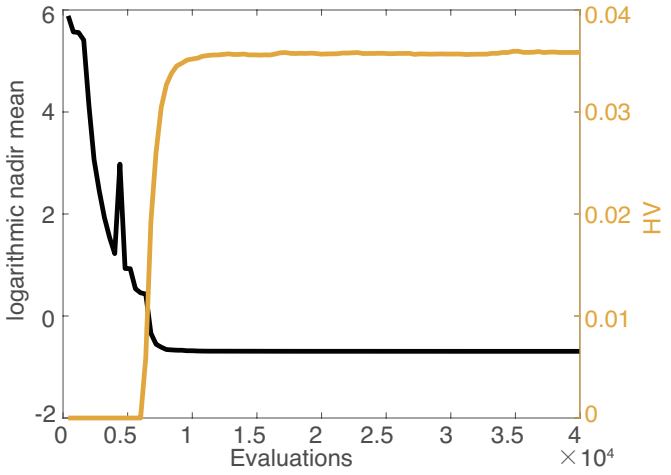

Fig. 4: Example of nadir point and hypervolume(HV) value on inverted-DTLZ1 3-dimension problem with FV-EMOA algorithm. The yellow curve is the change of hypervolume while the black curve is the change of logarithmic nadir point.

the early generations is larger than that near convergence. So we consider the logarithm. And considering the possible bad variance of the indicator, finally, we use the best logarithmic nadir point so-far as our indicator. more specifically, for a minimization problem, we consider the indicator as follows:

$$\begin{aligned} ENP_t &= [f_{t1}, f_{t2}, \ldots, f_{tm}]^\top \in \mathbb{R}^m, \\ I_0 &= \frac{1}{m}\sum_{i=1}^{m} lnf_{0i}, \\ I_t &= min(I_{t-1}, \frac{1}{m}\sum_{i=1}^{m} lnf_{ti}), t = 1, 2, \ldots, T, \end{aligned} \tag{5}$$

where T is the total number of generations, ENP_t is the estimated nadir point at the tth generation with m objectives $f_{t1}, f_{t2}, \ldots, f_{tm}$. I_0 is the initial indicator calculated by the initial population. And I_t is the minimum value before the tth generation (including the tth generation).

After chosen the indicator, the next step is to detect the stagnation of the indicator. We use a basic linear regression method called Simple Least Squares [24] with a simple least squares convergence detection strategy introduced in [18]. If the absolute value of the slope of the indicator is below a threshold, the convergence is reported. Briefly speaking, for a simple linear regression $I = a + bt$, the intercept a and slope b of the tth generation can be calculated with the following matrix-based formula:

$$\begin{bmatrix} a \\ b \end{bmatrix} = \begin{bmatrix} \sum t_i^2 & \sum t_i \\ \sum t_i & w\_l \end{bmatrix}^{-1} * \begin{bmatrix} \sum t_i * I_{t_i} \\ \sum I_{t_i} \end{bmatrix} \tag{6}$$

where w_l is the length of the chosen window and t_i is the evaluated number in the chosen window. The value of slope b is shown in Fig. 5 (Note that the value in the first w_l evaluations is 0, and we should not consider the first w_l evaluations).

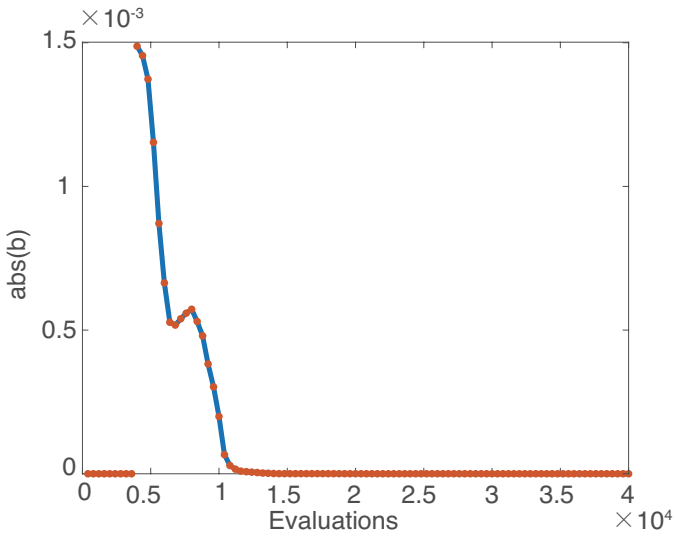

Fig. 5: Example of $|b|$ on inverted-DTLZ1 3-dimension problem (window size = 4000 evaluations with population size = 100).

With the above formula (6), the convergence detection criterion is defined as:

$$convergence = |b| < thres \tag{7}$$

The chosen of the $thres$ value is not so important as the report ahead or delay is not fatal to the algorithm or to the final solutions set. We choose the $thres$ value as 10^{-5} after some experimental computation with the window size $w\_l = 4000$ evaluations. If we do not change the window size, this threshold can be applied to other problems or indicator-based algorithms because of a weak convergence detection purpose.

V. Computational Experiments

To clearly represent the superiority of dynamically reference point adaptation and to ease the comparison process of two different dynamic mechanisms (linearly decrease mechanism and weak convergence detection mechanism), the mechanisms are going to be tested with the algorithm FV-EMOA [11]. The problems include: DTLZ series [25], WFG series [26] and their minus versions [27] and two inverted-triangular pareto front problems: Inverted-DTLZ1 [14], MaF1 [28]. To show the performance both on multi-objective and many-objective, we tested in 3 and 5 dimensions. All the code in this section is implemented in PlatEMO framework [29] with the following additional settings:

Population size: 100,
Total evaluation number: 400,000 solution evaluations,
Crossover: simulated binary (probability: 1.0),
Mutation: polynormal (probability: $1/n$),
Number of decision variables n:
$m + 4$ (DTLZ1, minus-DTLZ1, inverted-DTLZ1),
$m + 9$ (other problems),
Distribution index in Crossover and Mutation: 20,
Number of runs: 20 runs.

A. Computational Results

Each experiment has been run for twenty times independently. And the population size is 100, $r_{Initial} = 2$. The detailed algorithms are as following: FV-EMOA-2(the FV-EMOA [11] algorithm with the reference point adaptation with $r = 2$), FV-EMOA-Opt(the FV-EMOA algorithm with the reference point adaptation with $r = 1+1/H$), FV-EMOA-LD(the FV-EMOA algorithm with a linearly decrease mechanism), and FV-EMOA-CD(the FV-EMOA algorithm with a weak convergence detection mechanism, proposed in this paper). We obtain the hypervolume results after 40000 evaluations for each algorithm. The computational results is shown in TABLE I and TABLE II. The best result in each row is highlighted in bold, and relatively the worst result is shaded. The basic Wilcoxon signed-rank sum test is used in order to show the statistical significance for the algorithm comparing with FV-EMOA-CD proposed in this paper. The three symbols "+", "−", "≈" mean significantly better, significantly worse and no significant difference.

In the basic test problems(DTLZ1-4, WFG1, 2, 4 with the triangular pareto front except for WFG3), we can not tell the differences among the four algorithms in TABLE I, for that all the four algorithms are more or less the best or the worst and the Wilcoxon signed-rank sum tests show that almost all the results from the other three algorithms are not significantly different from FV-EMOA-CD (except 2 results from FV-EMOA-Opt are worse than results from FV-EMOA-CD).

But in the results of inverted-triangular pareto front problems (minus-DTLZ1-4, minus-WFG1-4, inverted-DTLZ1, 4, MaF1, 2), FV-EMOA-2 performs almost the worst in all experiments (23 out of 24), and the Wilcoxon signed-rank sum tests show that all the results from FV-EMOA-2 are significantly worse than FV-EMOA-CD. The reason is that the r is 2 all the process of FV-EMOA-2 algorithm. Comparing with FV-EMOA-CD, the final hypervolume values of FV-EMOA-Opt are not significantly different. And it is difficult to say FV-EMOA-CD is better than FV-EMOA-LD or vice versa, for that near one-third of results are better, one-third are worse, one-third are not significantly different.

B. The Importance of Using Dynamic Mechanism

We plot the final solutions distributions of some experiments including DTLZ4 and minus-DTLZ4 in 3-dimension (as shown in Fig. 6) and in 5-dimension (as shown in Fig. 7). The solutions distributions of Fig. 6a - 6c hint that the FVEMOA do not have good performance on concave pareto front problems. In Fig. 6d, the solutions are poor distributed comparing with Fig. 6a-6c. This phenomenon is also observed in Fig. 7d. The standard deviations of FV-EMOA-Opt on the DTLZ4 problem (shown in the TABLE I) are both higher than other three algorithms in 3- and 5-dimension($2.14e-1$ comparing with $1.21e-1, 1.31e-1, 1.76e-1$ in 3-dimension

TABLE I: HV mean and standard deviation over 20 independent runs for triangular pareto front problems.

Problem	M	D	FV-EMOA-2	FV-EMOA-Opt	FV-EMOA-LD	FV-EMOA-CD
DTLZ1	3	7	**1.4026e-1 (6.25e-5) ≈**	1.4020e-1 (1.14e-4) ≈	1.4021e-1 (1.15e-4) ≈	1.4022e-1 (7.38e-5)
DTLZ1	5	9	**4.8962e-2 (8.83e-6) ≈**	4.8955e-2 (1.55e-5) ≈	4.8957e-2 (1.35e-5) ≈	4.8952e-2 (2.06e-5)
DTLZ2	3	12	7.5684e-1 (1.10e-4) ≈	7.5683e-1 (1.48e-4) ≈	**7.5686e-1 (1.13e-4) ≈**	7.5681e-1 (1.32e-4)
DTLZ2	5	14	1.2934e+0 (3.12e-4) ≈	1.2934e+0 (2.65e-4) ≈	**1.2935e+0 (3.11e-4) ≈**	1.2935e+0 (2.62e-4)
DTLZ3	3	12	7.1789e-1 (7.31e-2) ≈	7.0047e-1 (1.65e-1) ≈	**7.4029e-1 (8.35e-3) ≈**	7.3655e-1 (9.43e-3)
DTLZ3	5	14	1.1264e+0 (3.87e-1) ≈	**1.1957e+0 (2.82e-1) ≈**	1.1351e+0 (3.89e-1) ≈	1.1931e+0 (2.84e-1)
DTLZ4	3	12	**6.9813e-1 (1.21e-1) ≈**	6.0515e-1 (2.14e-1) ≈	6.8340e-1 (1.31e-1) ≈	6.6637e-1 (1.76e-1)
DTLZ4	5	14	1.2381e+0 (9.98e-2) ≈	1.2308e+0 (1.01e-1) ≈	1.2424e+0 (7.21e-2) ≈	**1.2644e+0 (6.05e-2)**
WFG1	3	12	5.9236e+1 (9.45e-1) ≈	5.9204e+1 (7.24e-1) ≈	**5.9303e+1 (4.79e-1) ≈**	5.9298e+1 (8.50e-1)
WFG1	5	14	5.9946e+3 (3.02e+0) ≈	5.9908e+3 (1.09e+1) −	5.9801e+3 (6.90e+1) ≈	**5.9954e+3 (1.12e+0)**
WFG2	3	12	5.9711e+1 (1.94e-2) ≈	**5.9720e+1 (2.92e-2) ≈**	5.9712e+1 (2.54e-2) ≈	5.9703e+1 (3.49e-2)
WFG2	5	14	**6.0208e+3 (2.44e+0) ≈**	6.0170e+3 (4.04e+0) −	6.0186e+3 (3.72e+0) ≈	6.0195e+3 (5.24e+0)
WFG3	3	12	**6.6296e+0 (1.23e-2) ≈**	6.6238e+0 (1.16e-2) ≈	6.6222e+0 (9.24e-3) ≈	6.6229e+0 (1.46e-2)
WFG3	5	14	**3.3164e+0 (4.12e-2) ≈**	3.3137e+0 (3.46e-2) ≈	3.2991e+0 (3.42e-2) ≈	3.3105e+0 (3.46e-2)
WFG4	3	12	**3.6259e+1 (1.29e-2) ≈**	3.6252e+1 (2.87e-2) ≈	3.6258e+1 (1.43e-2) ≈	3.6251e+1 (2.37e-2)
WFG4	5	14	**4.9536e+3 (3.75e+0) ≈**	4.9503e+3 (3.64e+0) ≈	4.9531e+3 (2.55e+0) ≈	4.9523e+3 (2.25e+0)
$+/-/\approx$			0/0/16	0/2/14	0/0/16	

TABLE II: HV mean and standard deviation over 20 independent runs for inverted-triangular pareto front problems.

Problem	M	D	FV-EMOA-2	FV-EMOA-Opt	FV-EMOA-LD	FV-EMOA-CD
minus-DTLZ1	3	7	4.8083e+7 (1.08e+5) −	**4.9842e+7 (2.58e+4) ≈**	4.9832e+7 (2.04e+4) ≈	4.9842e+7 (2.51e+4)
minus-DTLZ1	5	9	5.6448e+11 (8.23e+9) −	8.5886e+11 (4.19e+9) ≈	8.3910e+11 (5.37e+9) −	**8.5919e+11 (5.29e+9)**
minus-DTLZ2	3	12	3.0452e+1 (3.82e-2) −	3.0690e+1 (7.55e-2) ≈	**3.0919e+1 (5.32e-2) +**	3.0696e+1 (9.18e-2)
minus-DTLZ2	5	14	8.5606e+1 (1.02e+0) −	1.0680e+2 (4.56e-1) ≈	**1.0766e+2 (3.15e-1) +**	1.0657e+2 (5.69e-1)
minus-DTLZ3	3	12	7.5985e+9 (7.41e+6) −	7.6308e+9 (2.89e+7) ≈	**7.7119e+9 (1.32e+7) +**	7.6232e+9 (3.43e+7)
minus-DTLZ3	5	14	8.5019e+15 (1.14e+14) −	1.0539e+16 (4.69e+13) ≈	**1.0603e+16 (7.31e+13) +**	1.0526e+16 (4.87e+13)
minus-DTLZ4	3	12	3.0434e+1 (3.77e-2) −	3.1092e+1 (2.34e-2) ≈	**3.1116e+1 (1.64e-2) +**	3.1089e+1 (2.57e-2)
minus-DTLZ4	5	14	8.4994e+1 (1.50e+0) −	**1.0797e+2 (1.95e-1) ≈**	1.0756e+2 (2.10e-1) −	1.0795e+2 (1.89e-1)
minus-WFG1	3	12	6.9856e+0 (2.77e-2) −	7.1742e+0 (4.52e-2) ≈	**7.1857e+0 (2.74e-2) +**	7.1844e+0 (3.78e-2)
minus-WFG1	5	14	1.4147e+1 (2.48e-1) −	**1.5635e+1 (2.33e-1) ≈**	1.5284e+1 (2.01e-1) −	1.5539e+1 (2.02e-1)
minus-WFG2	3	12	1.8711e+1 (1.19e-2) −	1.8965e+1 (4.48e-3) ≈	1.8958e+1 (4.32e-3) −	**1.8967e+1 (3.80e-3)**
minus-WFG2	5	14	4.7715e+1 (1.85e-1) −	**5.6183e+1 (1.78e-1) ≈**	5.5939e+1 (1.85e-1) −	5.6168e+1 (1.71e-1)
minus-WFG3	3	12	1.3765e+1 (3.31e-2) −	1.4269e+1 (9.29e-3) ≈	**1.4275e+1 (6.86e-3) ≈**	1.4274e+1 (7.04e-3)
minus-WFG3	5	14	4.2737e+1 (6.41e-1) −	6.3482e+1 (7.07e-1) ≈	6.2143e+1 (7.62e-1) −	**6.3513e+1 (6.15e-1)**
minus-WFG4	3	12	3.4059e+1 (4.33e-2) −	3.4700e+1 (4.83e-2) ≈	**3.4783e+1 (3.16e-2) +**	3.4725e+1 (5.17e-2)
minus-WFG4	5	14	6.2416e+2 (1.05e+1) −	7.9011e+2 (1.26e+0) ≈	7.8781e+2 (2.02e+0) −	**7.9023e+2 (1.63e+0)**
MaF1	3	12	2.8634e-1 (7.00e-4) −	**2.9746e-1 (1.36e-4) ≈**	2.9736e-1 (1.36e-4) ≈	2.9736e-1 (1.87e-4)
MaF1	5	14	1.1011e-2 (1.83e-4) −	1.6331e-2 (1.39e-4) ≈	1.6138e-2 (1.73e-4) −	**1.6331e-2 (9.90e-5)**
MaF4	3	12	4.0852e+1 (9.56e+0) −	3.9125e+1 (1.44e+1) ≈	4.1884e+1 (1.07e+1) ≈	**4.4345e+1 (2.82e+0)**
MaF4	5	14	3.7215e+3 (1.64e+3) −	**6.2601e+3 (2.81e+2) ≈**	6.2386e+3 (3.23e+2) ≈	6.1540e+3 (4.87e+2)
inverted-DTLZ1	3	7	3.5744e-2 (1.47e-4) −	3.6520e-2 (1.11e-3) ≈	**3.6961e-2 (2.51e-4) ≈**	3.6897e-2 (4.23e-4)
inverted-DTLZ1	5	9	3.1124e-4 (4.25e-5) −	**4.7494e-4 (4.71e-5) ≈**	4.5874e-4 (6.97e-5) ≈	4.2499e-4 (1.00e-4)
inverted-DTLZ2	3	12	7.0894e-1 (1.17e-3) −	7.1559e-1 (2.72e-3) ≈	**7.2070e-1 (1.16e-3) +**	7.1612e-1 (2.45e-3)
inverted-DTLZ2	5	14	1.6127e-1 (2.18e-3) −	2.0287e-1 (8.88e-4) ≈	**2.0452e-1 (6.98e-4) +**	2.0326e-1 (5.90e-4)
$+/-/\approx$			0/24/0	0/0/24	9/8/7	

and $1.01e-1$ comparing with $9.98e-2, 7.21e-2, 6.05e-2$ in 5-dimension). This observation also shows that the solutions distributions of some runs in FV-EMOA-Opt are poor over the total 20 runs.

In FV-EMOA-Opt, the algorithm applies $r_{Initial} = 1+1/H$ mechanism at the early stage of algorithm while other three algorithms apply $r_{Initial} = 2$. Even though the r_{final} of FV-EMOA-LD, FV-EMOA-CD and FV-EMOA-Opt are all equal to $1 + 1/H$, FV-EMOA-Opt can not jump out from the local minimum and estimate the pareto front well due to the pool searching behavior at the early stage.

The above examples clearly show the importance of using dynamic mechanism, that a slightly larger r than $1 + 1/H$ can make the algorithm with a better searching behavior in convergence stage where the solutions have not reached to the pareto front especially for the problems which are difficult to find the whole solutions space like the DTLZ4 problem.

C. Comparison of Two Dynamic Mechanisms

We want to further investigate the differences between two dynamic mechanisms (the linearly decrease mechanism and the weak convergence detection mechanism). Here are the examples of the final distribution on the MaF1 problem(as shown in Fig. 8). The total evaluation number is set to 3500 and the convergence is detected at 3400 evaluations. The solutions distribution of FV-EMOA-CD(Fig. 8c) is similar to the that of FV-EMOA-Opt(Fig. 8d) while there are still

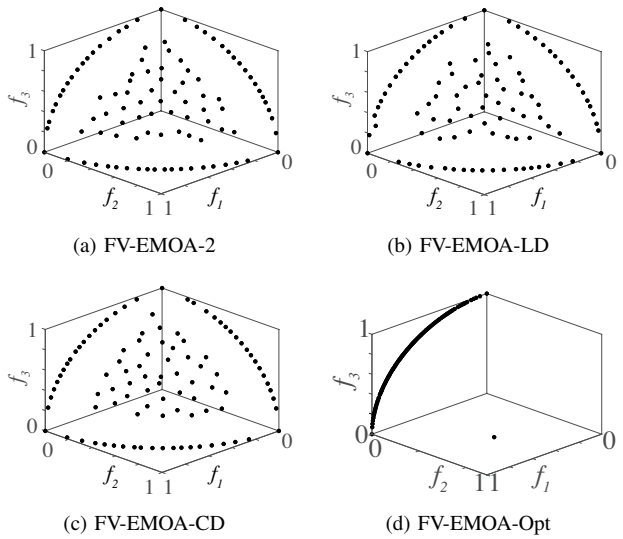

(a) FV-EMOA-2 (b) FV-EMOA-LD

(c) FV-EMOA-CD (d) FV-EMOA-Opt

Fig. 6: The final distribution of 4 reference point strategies on 3-dimensional DTLZ4 problems.

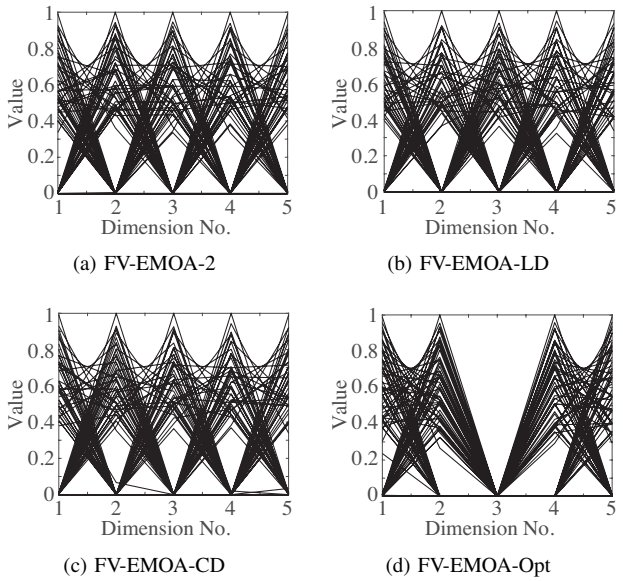

(a) FV-EMOA-2 (b) FV-EMOA-LD

(c) FV-EMOA-CD (d) FV-EMOA-Opt

Fig. 7: The final distribution of 4 reference point strategies on 5-dimensional DTLZ4 problems.

overmany solutions at the boundary of pareto front in FV-EMOA-LD(Fig. 8b).

The reason is quite intuitionistic. In the linearly decrease mechanism, the total evaluation number is so small that it is too late for the solutions to distribute evenly when reaching to the final generation. But in the weak convergence detection mechanism, a convergence is reported after 3400 evaluations and the algorithm still has 100 evaluations to make a good solutions distribution.

VI. Conclusions

In this paper, we emphasize the importance of reference point adaptation in indicator-based EMOA by a simple example. Then we state the dynamic reference point adaptation mechanism with the illustration by two aspects:

1) Optimal Distribution: Considering the flat triangular problems, the optimal setting of hypervolume reference point is $r = 1 + 1/H$.

2) Better Searching Behavior: In the early stage, the solutions may not be close to the true pareto front. A slightly larger value of r can achieve a better searching behavior especially on the problems which are difficult to find the whole objective space. We give an example of the DTLZ4 problem.

After that, a new dynamic reference point adaptation mechanism is proposed in this paper. A weak convergence detection mechanism is used. We apply our new dynamic mechanism on many test problems containing triangular, inverted-triangular pareto fronts problems. The results show that FV-EMOA with $r = 2$ performs the worst on the problems with inverted-triangular pareto fronts. FV-EMOA with weak convergence detection mechanism performs better or worse than FV-EMOA with linearly decrease mechanism but performs no significant difference comparing with FV-EMOA when $r = 1 + 1/H$.

We compare our new mechanism with the proposed linearly decrease mechanism and find that on some conditions, specifically the condition that the total evaluation number is limited to a small addition after the reported convergence, our weak convergence detection mechanism performs better than linear decrease mechanism especially on the problems with the small feasible region and easy mapping from decision space to objective space.

In the future, we plan to further investigate the behavior of our new mechanism. A larger dimensionality of MaOPs should be considered and the problems with different pareto front shapes should be tested and analyzed detailedly. Our weak convergence detection mechanism can also be further improved.

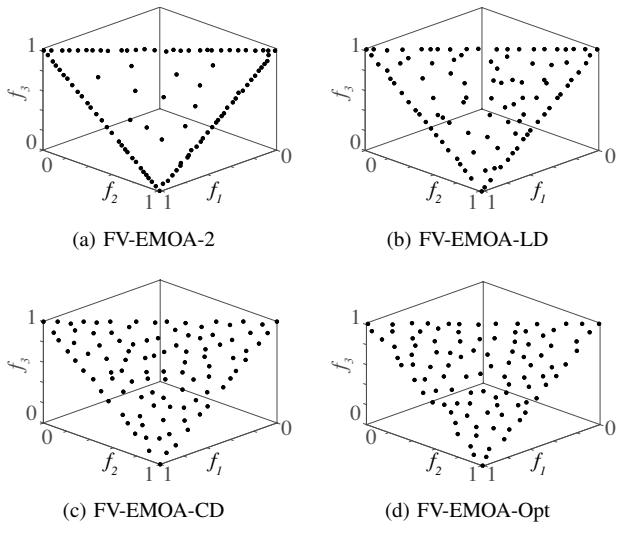

(a) FV-EMOA-2 (b) FV-EMOA-LD

(c) FV-EMOA-CD (d) FV-EMOA-Opt

Fig. 8: The final distribution of 4 reference point strategies on the MaF1 problem. The results are obtained after 3500 evaluations($t_{Convergent} = 3400$).

REFERENCES

[1] E. Zitzler and L. Thiele, "Multiobjective optimization using evolutionary algorithmsa comparative case study," in *International conference on parallel problem solving from nature*. Springer, 1998, pp. 292–301.

[2] M. P. Hansen and A. Jaszkiewicz, *Evaluating the quality of approximations to the non-dominated set*. IMM, Department of Mathematical Modelling, Technical Universityof Denmark, 1994.

[3] E. Zitzler, L. Thiele, M. Laumanns, C. M. Fonseca, and V. G. da Fonseca, "Performance assessment of multiobjective optimizers: An analysis and review," *Trans. Evol. Comp*, vol. 7, no. 2, pp. 117–132, Apr. 2003. [Online]. Available: http://dx.doi.org/10.1109/TEVC.2003.810758

[4] C. A. C. Coello and M. R. Sierra, "A study of the parallelization of a coevolutionary multi-objective evolutionary algorithm," in *Mexican International Conference on Artificial Intelligence*. Springer, 2004, pp. 688–697.

[5] E. Zitzler, D. Brockhoff, and L. Thiele, "The hypervolume indicator revisited: On the design of pareto-compliant indicators via weighted integration," in *International Conference on Evolutionary Multi-Criterion Optimization*. Springer, 2007, pp. 862–876.

[6] N. Beume, C. M. Fonseca, M. Lopez-Ibanez, L. Paquete, and J. Vahrenhold, "On the complexity of computing the hypervolume indicator," *IEEE Transactions on Evolutionary Computation*, vol. 13, no. 5, pp. 1075–1082, 2009.

[7] J. Bader and E. Zitzler, "Hype: An algorithm for fast hypervolume-based many-objective optimization," *Evolutionary computation*, vol. 19, no. 1, pp. 45–76, 2011.

[8] K. Shang, H. Ishibuchi, M.-L. Zhang, and Y. Liu, "A new r2 indicator for better hypervolume approximation," in *Proceedings of the Genetic and Evolutionary Computation Conference*, ser. GECCO '18. New York, NY, USA: ACM, 2018, pp. 745–752. [Online]. Available: http://doi.acm.org/10.1145/3205455.3205543

[9] A. Menchaca-Méndez, E. Montero, and S. Zapotecas-Martínez, "An improved s-metric selection evolutionary multi-objective algorithm with adaptive resource allocation," *IEEE Access*, vol. 6, pp. 63 382–63 401, 2018.

[10] N. Beume, B. Naujoks, and M. Emmerich, "Sms-emoa: Multiobjective selection based on dominated hypervolume," *European Journal of Operational Research*, vol. 181, no. 3, pp. 1653–1669, 2007.

[11] S. Jiang, J. Zhang, Y.-S. Ong, A. N. Zhang, and P. S. Tan, "A simple and fast hypervolume indicator-based multiobjective evolutionary algorithm," *IEEE Transactions on Cybernetics*, vol. 45, no. 10, pp. 2202–2213, 2014.

[12] H. Ishibuchi, R. Imada, S. Yu, and Y. Nojima, "How to specify a reference point in hypervolume calculation for fair performance comparison," *Evolutionary Computation*, vol. 26, no. 3, pp. 1–29, 2018.

[13] H. Ishibuchi, R. Imada, Y. Setoguchi, and Y. Nojima, "Reference point specification in hypervolume calculation for fair comparison and efficient search," in *Proceedings of the Genetic and Evolutionary Computation Conference*. ACM, 2017, pp. 585–592.

[14] ——, "Hypervolume subset selection for triangular and inverted triangular pareto fronts of three-objective problems," in *Proceedings of the 14th ACM/SIGEVO Conference on Foundations of Genetic Algorithms*. ACM, 2017, pp. 95–110.

[15] H. Ishibuchi, R. Imada, N. Masuyama, and Y. Nojima, "Dynamic specification of a reference point for hypervolume calculation in sms-emoa," in *2018 IEEE Congress on Evolutionary Computation (CEC)*. IEEE, 2018, pp. 1–8.

[16] ——, "Use of two reference points in hypervolume-based evolutionary multiobjective optimization algorithms," in *International Conference on Parallel Problem Solving from Nature*. Springer, 2018, pp. 384–396.

[17] H. Trautmann, U. Ligges, J. Mehnen, and M. Preuss, "A convergence criterion for multiobjective evolutionary algorithms based on systematic statistical testing," in *International Conference on Parallel Problem Solving from Nature*. Springer, 2008, pp. 825–836.

[18] J. L. Guerrero, L. Martí, A. Berlanga, J. García, and J. M. Molina, "Introducing a robust and efficient stopping criterion for moeas," in *IEEE Congress on Evolutionary Computation*. IEEE, 2010, pp. 1–8.

[19] T. Wagner, H. Trautmann, and B. Naujoks, "Ocd: Online convergence detection for evolutionary multi-objective algorithms based on statistical testing," in *International Conference on Evolutionary Multi-Criterion Optimization*. Springer, 2009, pp. 198–215.

[20] H. Trautmann, T. Wagner, B. Naujoks, M. Preuss, and J. Mehnen, "Statistical methods for convergence detection of multi-objective evolutionary algorithms," *Evolutionary computation*, vol. 17, no. 4, pp. 493–509, 2009.

[21] K. Deb and S. Jain, "Running performance metrics for evolutionary multi-objective optimization," 2002.

[22] O. Rudenko and M. Schoenauer, "A steady performance stopping criterion for pareto-based evolutionary algorithms," in *6th International Multi-Objective Programming and Goal Programming Conference*, 2004.

[23] T. Wagner, H. Trautmann, and L. Martí, "A taxonomy of online stopping criteria for multi-objective evolutionary algorithms," in *International Conference on Evolutionary Multi-Criterion Optimization*. Springer, 2011, pp. 16–30.

[24] W. Ericson, "Introductory probability and statistical applications," *Technometrics*, vol. 8, no. 4, pp. 720–722, 1970.

[25] K. Deb, L. Thiele, M. Laumanns, and E. Zitzler, "Scalable multi-objective optimization test problems," in *Proceedings of the 2002 Congress on Evolutionary Computation. CEC'02 (Cat. No. 02TH8600)*, vol. 1. IEEE, 2002, pp. 825–830.

[26] S. Huband, P. Hingston, L. Barone, and L. While, "A review of multiobjective test problems and a scalable test problem toolkit," *IEEE Transactions on Evolutionary Computation*, vol. 10, no. 5, pp. 477–506, 2006.

[27] H. Ishibuchi, Y. Setoguchi, H. Masuda, and Y. Nojima, "Performance of decomposition-based many-objective algorithms strongly depends on pareto front shapes," *IEEE Transactions on Evolutionary Computation*, vol. 21, no. 2, pp. 169–190, 2016.

[28] R. Cheng, M. Li, Y. Tian, X. Zhang, S. Yang, Y. Jin, and X. Yao, "A benchmark test suite for evolutionary many-objective optimization," *Complex & Intelligent Systems*, vol. 3, no. 1, pp. 67–81, 2017.

[29] T. Ye, C. Ran, X. Zhang, and Y. Jin, "Platemo: A matlab platform for evolutionary multi-objective optimization [educational forum]," *IEEE Computational Intelligence Magazine*, vol. 12, no. 4, pp. 73–87, 2017.